Invited Paper

JOURNAL OF THE CHINESE CHEMICAL SOCIETY

# Control of Catalytic Activity Via Porosity, Chemical Composition, and Morphology of Nanostructured Porous Manganese Oxide Materials

Chun-Hu Chen and Steven, L. Suib*

*Department of Chemistry, University of Connecticut, Storrs, CT 06269-3060, USA*

(Received: Nov. 17, 2011; Accepted: Nov. 28, 2011; Published Online: Dec. 8, 2011; DOI: 10.1002/jccs.201100699)

This review concerns a summary of synthesis, characterization, and applications of octahedral molecular sieve (OMS) materials. These OMS systems have been the focus of our research program for over 20 years. This review primarily covers the past 10 years with an emphasis on the most recent developments in this area. Some current areas of concern include the systematic synthesis of well ordered materials, control of particle sizes, generation of nano-size particles, and development of new synthetic methods like pulse laser deposition and epitaxial growth of oxidic materials. Applications include use of OMS in environmental catalysis, adsorption, clean energy materials, activation of the Greenhouse gas carbon dioxide, and selective oxidations. OMS catalysts are outstanding selective oxidation catalysts and can also drive total oxidations. The highly selective of OMS systems may be related to redox cycling and redox catalysis.

**Keywords:** Manganese oxides; Porous; Catalysis.

## INTRODUCTION

Porous materials are important for many catalytic systems, and have been extensively studied and applied in molecular catalysis and industry. These porous materials/molecular sieves, in terms of structural aspects, can be briefly classified to two different categories: octahedral and tetrahedral coordinated porous materials. For a long time, tetrahedral coordinated porous molecular sieves, composed of Si, Al or C, including zeolites, mesoporous silicates, clay materials, and others, are well investigated and used.[1,2] Their complex and adjustable structures, external/internal interconnections, acidity/basicity, porosity, functionality, and low cost make these tetrahedral catalysts or molecular sieves highly versatile in many fields.[3,4]

Recently, octahedral coordinated porous manganese oxide materials have attracted a great deal of attention due to their controllable structures, porosities, and catalytical selectivities in relation to those of tetrahedral porous materials.[5,6] In addition, manganese is one of the few elements which have more than five different stable oxidation states. This unique nature results in the valuable mixed-valency of the porous manganese oxide and greatly distinguishes this type of material from tetrahedral molecular sieves. First, the manganese oxide octahedral molecular sieves (OMS) are natural semiconductor materials, and they also possess unique properties that only come with transition metal and/or d-orbitals, which are generally not available in the tetragonal molecular sieve systems. Second, since transition metals are well known as the active centers/species in many artificial and natural/biological catalytical systems, the transition-metal based OMS promises a simpler and more effective incorporation of various other transition metal active species. These superior advantages have raised many useful applications of manganese oxide OMS in catalysis, semiconductors, ion-exchange, radioactive-hazard separation, sensors, and batteries.[5,7-15]

Environmental protection is an important issue in this century. There are data showing that human civilization activities have significantly affected, or even damaged, the equilibrium and sustainability of the Earth irreversibly. One of our recent research directions is to explore the application and usages of OMS materials on the issues of environment protection. Solutions for water cleaning, recycling of the green-house gas $CO_2$, and sustainable energy materials are urgent research tasks. OMS materials have shown a highly selective oxidation with remarkable catalytic activities, especially alcohol oxidation towards aldehyde products.[16] Excellent catalytic performance inspires the application of OMS catalysts for environmental protection. In addition, high catalytic selectivity is the key to saving large amounts of time and energy on product separation/purification in industry. Investigation of highly selective OMS catalysts would provide the opportunity of conducting highly energy-efficient chemical engineering to generate products with lower energy input and less $CO_2$ emission.

* Corresponding author. E-mail: steven.suib@uconn.edu

  

In this review, the recent research progress of OMS materials on the issues of environmental pollution cleaning, clean energy materials, green house gas ($CO_2$) treatment/reuse with respect to the morphological and compositional control of OMS is summarized. The highly selective molecular catalysis of OMS, important for energy-saving catalysis, is also included. The general background and current focuses regarding control synthesis, nanoscale structures, and catalytic results of OMS materials are also discussed.

## STRUCTURES AND PREPARATION OF MANGANESE OXIDE MATERIALS

For years, our research interests of manganese oxide focus on preparing various octahedral molecular sieves (OMS), octahedral layer (OL), and also amorphous manganese oxide (AMO) materials, mainly with a mixed valency system of $Mn^{4+}$ and $Mn^{3+}$.[6,17-19] In these OMS materials, the $MnO_6$ octahedron building blocks are connected by vertices and edges, generating various porous tunnel structures.[20,21] The schematic structural presentation and chemical compositions of several common OMS and OL materials are shown in Fig. 1 and Table 1, respectively. Positive-charge ions are present inside the tunnels or interlayer to compensate the negative charge caused by the mixed valency of $Mn^{4+}$ and $Mn^{3+}$. The ion exchange of these tunnel or interlayer ions is important for applications of catalysis, batteries, and ion traps. For example, $Mg^{2+}$ ions commonly occupy the 3 × 3 tunnel of the synthetic OMS-1 (Fig. 1a),[22] and $K^+$ ions for 2 × 2 tunnel in OMS-2 (Fig. 1b).[23] These interlayer cations, (also $Rb^+$, $Na^+$, $Li^+$, and other cationic organic surfactants)[24,25] have been considered as structure directors of tunnel size and structure control in porous manganese oxides, although this hypothesis is not always true in some studies. Typically, the OL materials (eg. birnessite) are used as the precursors and ion-exchange is conducted to place desired cations into the interlayer spacing. The strong charge density in the OL materials requires a 3-4 step process to complete the intercalation/ion-exchange of desired ions.[18,26,27] These modified OL precursors can then be converted into tunnel structures under different synthetic conditions, normally involving high temperatures and pressure. This structural transformation method provides a general route toward various manganese oxide products with desired tunnel sizes, structures, and phases. Some OMS materials can only be prepared through this multi-step procedure. Due to the versatility and demand of OL precursors, Chen *et al.* have recently reported a rapid single-step preparation to produce highly-ordered, intercalated OL materials with large interlayer spacing (Scheme I), in which the synthesis of intercalated OL precursors can be significantly simplified.[25]

Although the intercalated OL precursors can be prepared easily, these multi-step structural transformation methods generate impurities, require longer preparation times, complicated operations, and are not able to provide promising control of specific morphologies and particle sizes. One of our main research directions is to explore single-step preparation and size-, shape-, structure-specific syntheses of OMS materials.[28-30] These single-step procedures certainly provide more reliable controls of morphology, shape, and properties of materials, yet only one specific product can be produced, which may not be as versatile or general as the structural transformation preparations.

### Morphology Control of Nanostructured OMS-2

OMS-2 materials with open 2 × 2 tunnels have been widely studied due to outstanding catalytic applications. Studies have shown that the catalytic performance is highly

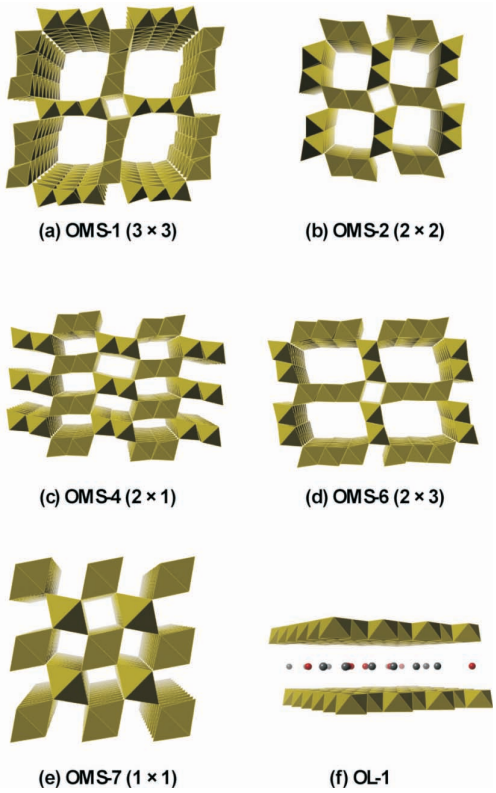


Fig. 1. Schematic structures of several common porous manganese oxide OMS and OL materials.

  

Table 1. Compositions and structures of common OMS materials

| Materials | Structures | Composition | Mineral Name |
|---|---|---|---|
| OMS-1 | 3 × 3 | $Mg^{2+}_{1.9\text{-}1.94}Mn^{2+}_{0.9\text{-}1.4}Mn^{4+}_{4.4\text{-}4.5}O_{12}\cdot nH_2O$ | Todorokite |
| OMS-2 | 2 × 2 | $K_xMnO_2\cdot nH_2O$ | Cryptomelane |
| OMS-4 | 2 × 1 | $MnO_2$ | Ramsdellite |
| OMS-6 | 2 × 3 | $(Na,H_2O)_xMn_5O_{10}$ | Romanechite |
| OMS-7 | 1 × 1 | $MnO_2$ | Pyrolusite |
| OL-1 | Layered structure | $K_{0.25\text{-}0.45}MnO_2\cdot nH_2O$ | Birnessite |

**Scheme I** The single-step procedure for large-interlayer spacing OL materials. Reproduced with permission from Ref. 25. Copyright 2008 American Chemical Society

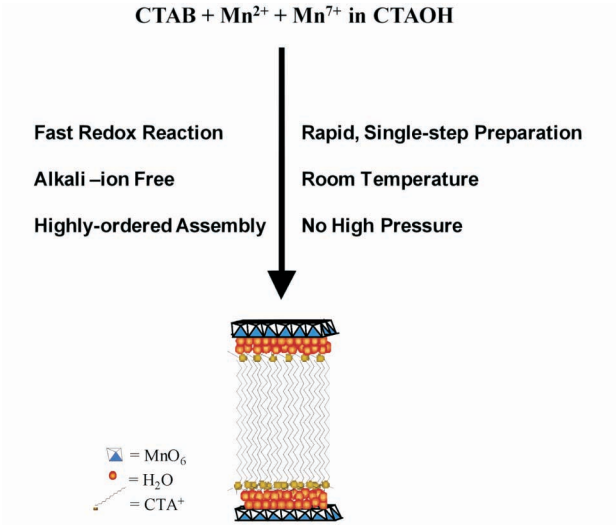


affected by the preparation methods.[31] While different temperatures, pressure, and pH are important for the controls of morphology and sizes, synthetic approaches, including hydrothermal,[32,33] laser deposition,[34] microwave,[35] air-oxidation,[36] reflux,[23] sol-gel,[37] doping,[38,39] solid-state reaction,[40] and others, were carried out in our group to enhance the performance of OMS-2 for various applications.

Typical preparations involve reduction of $Mn^{7+}$, oxidation of $Mn^{2+}$, or the combined one-step redox reaction of $Mn^{7+}$ and $Mn^{2+}$. In the sol-gel synthesis, hydrocarbon compounds are commonly used as the reducing reagents to interact with permanganate to produce OMS-2 materials.[37] To oxidize $Mn^{2+}$ into OMS-2, proper selection of oxidants, such as dichromate, persulfate, hydrogen peroxide, and others, was reported as an effective route toward shape and size control of OMS-2 materials.[33,41,42] The reflux methods in aqueous systems are also widely used (Eq. 1).

$$2MnO_4^-{}_{(aq)} + 3Mn^{2+}{}_{(aq)} + 2H_2O_{(l)} \rightarrow 5MnO_{2(s)} + 4H^+ \quad (1)$$

Nanorod-like OMS-2 materials are commonly generated by mild reflux treatment in water (Fig. 2). This approach is also popular for the synthesis of doped-OMS-2 materials. Nyutu *et al.* have shown that microwave-assisted reflux can significantly control the width of fibrous rods down to a few nanometers.[35] In terms of length control, the hydrothermal method tends to produce much longer OMS-2 nanowires up to several hundred microns in length under higher temperatures and pressure as compared to the reflux method.[33] Dendritic OMS-2 with highly uniform square cross-section fibers can also be prepared with hydrothermal methods.[42] These dendritic OMS-2 materials were then used as structural templates for shape controlled syntheses of other materials via epitaxy.[43] Except for liquid phase preparations, the new excitement of stoichiometry-specific deposition of structural and compositional complex OMS-2 has been realized by pulse laser deposition techniques with the critical control of oxygen levels during the deposition process.[34]

Highly thermal stable OMS-2 materials are essential for high-temperature catalytic systems. The typical thermal stability of the OMS-2 phase prepared by the previously mentioned methods is around 500-550 °C in air. Cai and Jin *el al.* reported the two-step air oxidation method to produce

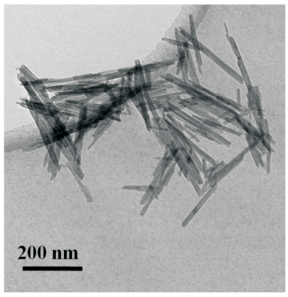


Fig. 2. The TEM image of nanostructured OMS-2 produced by reflux treatment in water.

  

highly stable K-OMS-2 with a thermal stability up to around 800 °C, further expanding the application window of OMS-2 materials.[44,45]

## POROSITY

The BET surface area of porous manganese oxide materials is highly dependent on the preparation procedures, generally within the range of 50-250 $m^2g^{-1}$. Mesopores and micropores are observed in both manganese oxide octahedral molecular sieves and layered materials. For example, in OMS-2 materials, the double-wide slab is 4.6 Å with a diagonal across 2 × 2 open about 6.5 Å, which is a typical microporous system. However, studies for many years have only suggested the presence of micropores with a small amount of micropore volume. This is mainly due to the diffusion limit of nitrogen molecule in porosity studies at liquid nitrogen temperature (77 K). Similar difficulties have been reported in other microporous zeolite materials. Recently Luo *et al.* reported success in experimental probing of micropores in OMS and layered materials using $CO_2$ at 273K.[46] These results are important to clarify the argument of the pore-size dependent selectivity with OMS catalysts.

## MOLECULAR CATALYSIS AND SELECTIVITY OF OMS MATERIALS

### Selective Oxidation of Alcohol

The control of selective alcohol oxidation to aldehyde with simple and one-step processes remains a challenge. Few systems can utilize only one catalyst without any additives to selectively stop the oxidation at the aldehyde stage. Aldehydes are valuable intermediates for many pharmaceutical and organic syntheses. The first demonstration reported by Son *et al.* regarding highly selective oxidation of benzyl alcohols in the liquid phase with the presence of K-OMS-2 or protonated OMS-2 (H-K-OMS-2) shows 100% selectivity to aldehydes with more than 90% conversion (Scheme II).[16] This report presents the role of OMS-2 materials as highly efficient and selective catalysts capable of uptaking molecular oxygen in air as an oxidant to complete a one-pot oxidation. Later, the detailed catalytic mechanism of selective alcohol oxidation was investigated by Makwana *et al.* using $^{18}O$ isotope-labeling (Scheme III).[47] The results confirm that OMS-2 catalysts utilize molecular oxygen as an oxidant in a two-step Mars-van Krevelen model regarding the exchange between gas and lattice oxygen in the cycle. The occurrence of a two-electron redox cycle in manganese species (between $Mn^{2+}$ and $Mn^{4+}$) is associated with two-electron reduction of molecular oxygen to hydrogen peroxide.

**Scheme II** The highly-selective oxidation of alcohol via OMS-2 catalysts

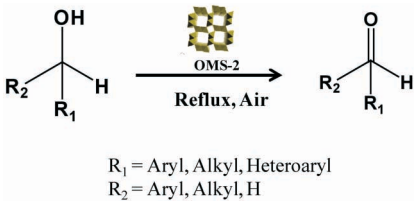


**Scheme III** The catalytic mechanism of benzyl alcohol oxidation with molecular oxygen and OMS-2 catalysts

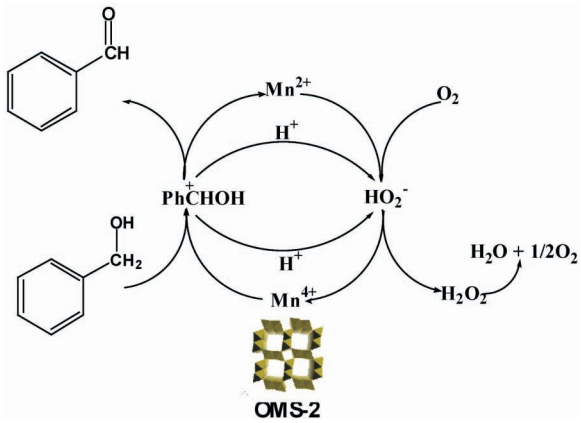


### Carbon-Hydrogen Bond Oxidation

After the exploration of the alcohol oxidation by OMS-2 materials, studies of carbon-hydrogen bond oxidation were conducted to further understand the oxidation capacity of OMS materials. Opembe *et al.* studied the oxidation of 9H-fluorene catalyzed by OMS-2 with molecular oxygen into 9-fluorenone without any additives.[48] High selectivities (95-100%) with excellent conversions, 4-99% conversions, both highly dependent on the solvent environment, were reported. The studies of kinetics, kinetic isotope effect, and catalyst preparations were also presented. The mechanisms propose that the C-H cleavage is the rate-controlling step and a free-radical mechanism is involved (Scheme IV), which is different from the mechanism of benzyl alcohol oxidation.

Jin *et al.* reported another success of C-H oxidation of toluene with porous OMS under mild conditions.[29] Although the methyl group in toluene is at the allylic site, to-

  

**Scheme IV** The radical mechanism of 9H-fluorene oxidation using OMS-2. Reproduced with permission from Ref. 48. Copyright 2008 Wiley and Sons

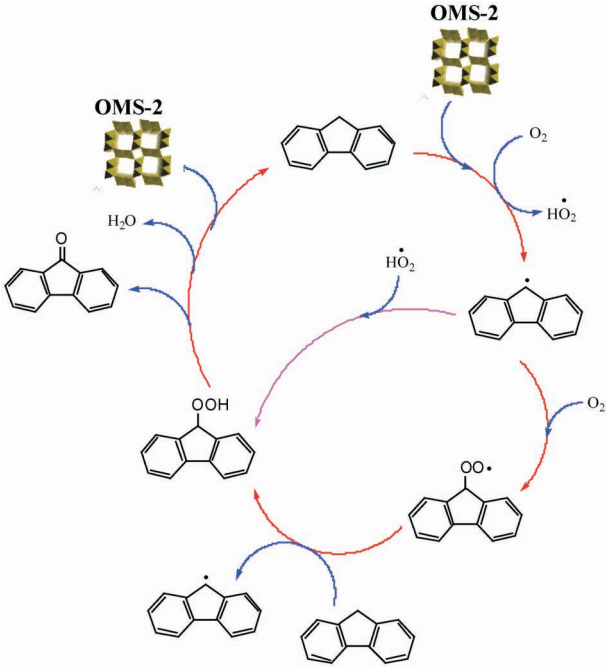


luene is a stable and inert solvent compound in organic reactions. This work significantly challenges the oxidative activity of OMS catalysts in the liquid phase via only the oxygen in air without any pressurized reaction conditions. The results show that OMS-2 catalysts give an excellent 100% selectivity to benzoic aldehyde but low conversion (< 1%), while the other OMS catalyst, γ-$MnO_2$, having a disordered 1 × 1 (pyrolusite, OMS-7) and 1 × 2 (ramsdellite, OMS-4) tunnel structures, gives the highest conversions with 15% and 57% selectivities to benzoic aldehyde and benzoic acid, respectively.

The uniform tunnel size in catalysts, like OMS-2, could be responsible for the highly selective oxidation. Similar to the mechanism of 9H-fluorene oxidation, the toluene oxidation by OMS is through a free-radical pathway. These results show that two different oxidation routes by OMS materials: carbon-hydrogen bond oxidation involves the free-radical pathway and alcohol oxidation goes through two-electron redox reactions.

## APPLICATION OF OMS MATERIALS FOR ENVIRONMENTAL PROTECTION

### Catalytic Activation and Recycle of $CO_2$

The global warming caused by the greenhouse effect has extensively impacted our climate today and has become a significant threat of all the living species on the Earth. The dramatic increase of carbon dioxide concentrations in the atmosphere over the past several decades has been considered as one of the major reasons of global warming. Due to the unique mix-valency, outstanding selectivity, and low cost of OMS-2, we attempt to explore the application of these materials to activate and/or recycle $CO_2$ as oxygen and carbon sources to produce other valuable hydrocarbons.

To mimic Nature photosynthesis of $CO_2$ activation and water splitting together for hydrocarbons, Hu *et al.* have combined electrocatalysis and thermal activation to produce paraformaldehyde with nearly 100% selectivity by feeding $CO_2$ and $H_2O$ over metal/metal oxide catalyst systems.[49] The metal oxide layer acts as the oxygen ion conductor to assist the reduction of $CO_2$ and $H_2O$ on the Pt surface. The results also show that using OMS-2 as a metal oxide support can significantly decrease the reaction temperatures from around 900 °C (using calcia stabilized zirconia) to the range of 250-450 °C. This achievement is due to the unique bifunctionality of OMS-2 as an ion conductor and mixed-valency semiconductor, especially advantageous in this electrocatalytic system as compared to other single functionality metal oxide materials.

An example of $CO_2$ recycling to perform ethane dehydrogenation with $CO_2$, instead of using oxygen over OMS-2 catalysts to generate ethylene and CO for industrial carbonylation (Eq. 2) has bene done. Jin and coworkers have revealed that OMS-2 catalysts can significantly enhance the conversion and selectivity toward ethylene, with much higher $CO_2$ consumption (56%), as compared to that of a conventional chromium oxide system (< 20%), within a short time.[36] The presence of $CO_2$ can even further prevent coke deposition on the catalysts and give a remarkable continuous catalytic stability longer than 24 hours, which is highly valuable for practical industrial applications. A detailed reaction mechanism shows that two reactions are involved (Eq. 3 and 4). The active OMS-2 catalyzes the ethane independently to generate ethylene and hydrogen. The reverse water-gas shift reaction, also catalyzed by OMS-2, consumes the as-generated hydrogen to reduce the chance of side product (ie. methane) formation. As the reaction temperatures are required to be 700-800 °C, most OMS-2 materials prepared via one-step methods with thermal stability around 500 °C are not able to survive under such circumstances. The OMS-2 catalysts in this work

  

must be specially prepared by thermal structural transformation from birnessite at 800 °C, again showing that the physical and catalytic properties of OMS materials are highly dependent on the preparation methods. The overall mechanism of the $CO_2$ reforming of ethane is shown below in Equations 2-4.

$$C_2H_{6(g)} + CO_{2(g)} \rightarrow C_2H_{4(g)} + CO_{(g)} + H_2O_{(g)} \quad (2)$$
$$C_2H_{6(g)} \rightarrow C_2H_{4(g)} + H_{2(g)} \quad (3)$$
$$H_{2(g)} + CO_{2(g)} \rightarrow CO_{(g)} + H_2O_{(g)} \quad (4)$$

**Water Cleaning**

Clean water is currently an important international issue in many countries. Public health and resources, infectious disease, and medical-care spending are all dependent on the quality of water. One major challenge of water cleaning is that many toxic species can not be easily separated from water. Direct decomposition of methylene blue dye in water by Sriskandakumar *et al.* with the presence of oxidants has shown that OMS-2 materials are highly active on cleaning dye molecules in aqueous systems.[50] The Mo incorporated K-OMS-2 materials can quickly decompose dyes three times faster than that of non-modified K-OMS-2. Recently, Hu *et al.* demonstrated the removal of phenol in water using transition-metal doped OMS-2 nanofibers.[51] The relative high solubility of phenol in water causes a significant phenol accumulation in surface water, ground water, and soil. The OMS-2 doped with $Cu^{2+}$, $Co^{3+}$, and $Ce^{4+}$ show both enhanced adsorption capacity and oxidative activity than non-modified OMS-2. The scanning electron microscopy images show a clear adsorption of organic spheres on the surface of catalysts (Fig. 3). Large surface area samples generally show better efficiency than small surface area samples, suggesting that adsorption plays an important role in oxidative decomposition. The control adsorption experiments performed in an inert nitrogen atmosphere demonstrate that oxygen molecules significantly enhance the phenol adsorption and oxidation.

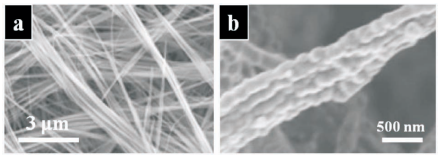


Fig. 3. The SEM images of the adsorption of organic spheres on the surface of OMS-2 catalysts. (a) The pristine OMS-2 catalysts, and (b) the adsorption of organic spheres. Reproduced with permission from Ref. 49. Copyright 2010 American Chemical Society.

Besides the contaminants existing inside water, large-area spills of oil or organic contaminants on water surfaces are always severe disasters for water cleaning and the ecological system. The main difficulty is how to clean the large-area organic contaminants efficiently. Selective adsorption of polar molecules from contaminated water by OMS-2 nanowire membranes promises a potential solution for this issue.[52] These unique membranes are assembled by OMS-2 nanowires and engineered into paper-like membranes. The membrane surface can be reversibly modified with hydrophobic polymers to create superwetting properties, contributing to a highly selective adsorption towards oil/organic contaminants. The capacity of this "super-adsorbance" can adsorb organic contaminants around 20 times the membrane weight, much superior as compared to those of porous polymer and silicon-coated glass membranes. Together with the low production cost, the OMS-2 membranes have a distinct possibility for applications of efficient cleaning of water.

**CO Removal**

The presence and emission of CO is important in automobile/industry emissions, battle fields, fire scenes, fuel cells, and others. Fast CO detoxification/oxidation is a highly urgent and challenging topic that requires catalysts with high capacity, low-temperature activity, and inexpensive cost. Although amorphous manganese oxide (AMO) is generally considered to have no long range order of particular tunnel structures, the large surface area with the nature of mixed-valency allows this material to be a highly active catalyst in many systems to perform fast, stable, and high conversion catalysis at relatively low temperatures. To achieve the success of using AMO as an environmental CO cleaning catalysts, surface and/or structural functionalizations are necessary to use this catalyst under many practical conditions with elongated lifetime and enhanced performance. Chen and Nijagi have currently been focusing on modifying the AMO catalyst for moisture- and hydrogen-rich conditions.[53] The hydrophobic polydimethylsiloxane (PDMS) surface coating on AMO successfully protects the active sites from environmental moisture, allowing a wide usage of this PDMS-coated AMO in many practical conditions. In addition, the copper incorporated AMO catalysts also show exceptional CO oxidation activities at low temperatures and a highly selective oxidation toward CO under a hydrogen-rich environment due to the dif-

  

ferent activation energy between CO and hydrogen at low temperatures, which is highly favorable for polymer electrolyte membrane (PEM) fuel cells.[54,55]

**Epitaxy for Energy Materials**

Nanostructured $TiO_2$ is a versatile clean energy material widely used in solar cells, water splitting, and other energy harvesting technologies.[56] The epitaxy based on OMS-2 materials toward 3D nanostructured $TiO_2$ was recently revealed with a simple and low-cost approach.[43] The unique superstructures are composed of approximately 25-nm-thick shell and ultrafine nanofibers (5-10 nm diameter) above the shell (Fig. 4). Various nanostructures (eg. nanotubes, nanorods, superstrcutres, etc.) can be selectively prepared through controls of substrates, precursor concentrations, and reaction conditions. The detailed characterization indicates that the epitaxial misfits and interfacial energy lead to the formation of unique nanoscale superstructures. Experimental results suggest that this concept could be general for the production of nanoscale materials. This technique was successfully applied to produce nanoscale antenna-like $TiO_2$ on substrates, the highly ordered array and large surface are both desired for clean energy and applications of photocatalysis, solar cells, and sensors.

## CONCLUSION

In this review, the great potential of using porous manganese oxide materials for $CO_2$ recycling, water clean-up, CO removal, nanostructured energy materials, and selective catalysis are demonstrated. The properties and performance of OMS materials for these applications are highly dependent on the preparation methods and conditions. Control of thermal stability, morphology, sizes, self-assembly, phase/structure, porosity, structural doping, and conductivity can be achieved with a proper selection of synthetic routes. The adjustable, room-temperature stable mixed-valency in OMS materials allows flexible electron transfer and reaction activation, leading to a wide range of applications. In particular, $CO_2$ reuse/recycling have opened the new possibility of using the oxidative catalysts like OMS to convert highly oxidized and inert molecules into other valuable molecules with less input energy. These advantages rival tetrahedral-coordinated porous materials and lead to new ideas and strategies for new challenges. In the near future, new functionalities and performance of OMS materials will be pursued via novel, simple, and low-cost synthetic methods. Continuous effort on more environmental protection issues, selective catalysis, and energy materials will be emphasized.

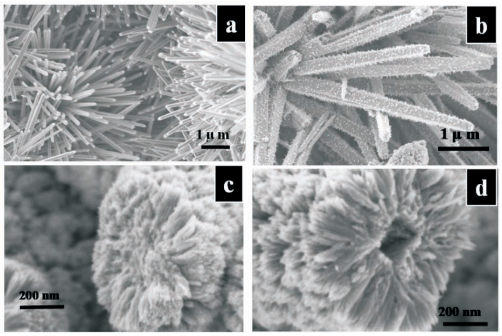


Fig. 4. The nanostructured $TiO_2$ heteroepitaxial growth on OMS-2. (a) The pristine OMS-2. (b) The nanostructured $TiO_2$ features on the OMS-2. (c) The larger amount of $TiO_2$ deposition on OMS-2, as compared to that in (b). (d) The nanostructured $TiO_2$ after the removal of OMS-2 core from (c). The square cross-section of the etched OMS-2 is clearly shown.

## ACKNOWLEDGEMENTS

We acknowledge the support from Department of Energy, Office of Basic Energy Sciences, Division of Chemical Sciences, Geosciences, and Biosciences under Grant **DE-FG02-86ER13622.A000** for our research of porous manganese oxide materials.

## REFERENCES

1. Corma, A. *Chem. Rev.* **1997**, *97*, 2373-2419.
2. Davis, M. E. *Nature* **2002**, *417*, 813-821.
3. Moller, K.; Bein, T. *Chem. Mater.* **1998**, *10*, 2950-2963.
4. Sakamoto, Y.; Kaneda, M.; Terasaki, O.; Zhao, D. Y.; Kim, J. M.; Stucky, G.; Shim, H. J.; Ryoo, R. *Nature* **2000**, *408*, 449-453.
5. Feng, Q.; Kanoh, H.; Ooi, K. *J. Mater. Chem.* **1999**, *9*, 319-333.
6. Suib, S. L. *Acc. Chem. Res.* **2008**, *41*, 479-487.
7. Lin, Y. H.; Cui, X. L.; Li, L. Y. *Electrochem. Commun.* **2005**, *7*, 166-172.
8. Jin, L.; Xu, L. P.; Morein, C.; Chen, C. H.; Lai, M.; Dharmarathna, S.; Dobley, A.; Suib, S. L. *Adv. Funct. Mater.* **2010**, *20*, 3373-3382.
9. Giovanoli, R.; Balmer, B. *Chimia* **1981**, *35*, 53-55.
10. Espinal, L.; Suib, S. L.; Rusling, J. F. *J. Am. Chem. Soc.* **2004**, *126*, 7676-7682.
11. Calvert, C.; Joesten, R.; Ngala, K.; Villegas, J.; Morey, A.; Shen, X.; Suib, S. L. *Chem. Mater.* **2008**, *20*, 6382-6388.
12. Chen, H. M.; He, J. H.; Zhang, C. B.; He, H. *J. Phys. Chem. C* **2007**, *111*, 18033-18038.
13. Shen, Y. F.; Zerger, R. P.; Deguzman, R. N.; Suib, S. L.; McCurdy, L.; Potter, D. I.; Oyoung, C. L. *Science* **1993**, *260*,

  

511-515.
14. Feng, Q.; Kanoh, H.; Miyai, Y.; Ooi, K. *Chem. Mater.* **1995**, *7*, 1722-1727.
15. Post, J. E. *Proc. Nal. Acad. Sci. U. S. A.* **1999**, *96*, 3447-3454.
16. Son, Y.-C.; Makwana, V. D.; Howell, A. R.; Suib, S. L. *Angew. Chem., Int. Ed.* **2001**, *40*, 4280-4283.
17. Chen, C.-H.; Abbas, S. F.; Morey, A.; Sithambaram, S.; Xu, L.-P.; Garces, H. F.; Hines, W. A.; Suib, S. L. *Adv. Mater.* **2008**, *20*, 1205-1209.
18. Ma, Y.; Suib, S. L.; Ressler, T.; Wong, J.; Lovallo, M.; Tsapatsis, M. *Chem. Mater.* **1999**, *11*, 3545-3554.
19. Liu, Z.-h.; Ooi, K.; Kanoh, H.; Tang, W.-P.; Tomida, T. *Langmuir* **2000**, *16*, 4154-4164.
20. Gao, T.; Glerup, M.; Krumeich, F.; Nesper, R.; Fjellvag, H.; Norby, P. *J. Phys. Chem. C* **2008**, *112*, 13134-13140.
21. Brock, S. L.; Duan, N.; Tian, Z. R.; Giraldo, O.; Zhou, H.; Suib, S. L. *Chem. Mater.* **1998**, *10*, 2619-2628.
22. Tian, Z. R.; Yin, Y. G.; Suib, S. L.; Oyoung, C. L. *Chem. Mater.* **1997**, *9*, 1126-1133.
23. DeGuzman, R. N.; Shen, Y.-F.; Neth, E. J.; Suib, S. L.; O'Young, C.-L.; Levine, S.; Newsam, J. M. *Chem. Mater.* **1994**, *6*, 815-821.
24. Liu, J.; Makwana, V.; Cai, J.; Sui, S. L.; Aindow, M. *J. Phys. Chem. B* **2003**, *107*, 9185-9194.
25. Chen, C.-H.; Crisostomo, V. M. B.; Li, W.-N.; Xu, L.; Suib, S. L. *J. Am. Chem. Soc.* **2008**, *130*, 14390-14391.
26. Liu, Z.-H.; Tang, X.; Zhang, C.; Zhou, Q. *Chem. Lett.* **2005**, *34*, 1312-1313.
27. Omomo, Y.; Sasaki, T.; Wang, L.; Watanabe, M. *J. Am. Chem. Soc.* **2003**, *125*, 3568-3575.
28. Huang, H.; Chen, C. H.; Xu, L. P.; Genuino, H.; Garcia-Martinez, J.; Garces, H. F.; Jin, L.; Kithongo, C. K.; Suib, S. L. *Chem. Commun.* **2010**, *46*, 5945-5947.
29. Jin, L.; Chen, C.-H.; Crisostomo, V. M. B.; Xu, L.; Son, Y.-C.; Suib, S. L. *Appl. Catal., A* **2009**, *355*, 169-175.
30. Shen, X.; Ding, Y.; Liu, J.; Laubernds, K.; Zerger, R. P.; Polverejan, M.; Son, Y.-C.; Aindow, M.; Suib, S. L. *Chem. Mater.* **2004**, *16*, 5327-5335.
31. Liu, Z.; Xing, Y.; Chen, C.-H.; Zhao, L.; Suib, S. L. *Chem. Mater.* **2008**, *20*, 2069-2071.
32. Li, W.-N.; Yuan, J.; Gomez-Mower, S.; Sithambaram, S.; Suib, S. L. *J. Phys. Chem. B* **2006**, *110*, 3066-3070.
33. Yuan, J.; Laubernds, K.; Villegas, J.; Gomez, S.; Suib, S. L. *Adv. Mater.* **2004**, *16*, 1729-1732.
34. Espinal, A. E.; Zhang, L. C.; Chen, C. H.; Morey, A.; Nie, Y. F.; Espinal, L.; Wells, B. O.; Joesten, R.; Aindow, M.; Suib, S. L. *Nat. Mater.* **2009**, *9*, 54-59.
35. Nyutu, E. K.; Chen, C.-H.; Sithambaram, S.; Crisostomo, V. M. B.; Suib, S. L. *J. Phys. Chem. C* **2008**, *112*, 6786-6793.
36. Jin, L.; Reutenauer, J.; Opembe, N.; Lai, M.; Martenak, D. J.; Han, S.; Suib, S. L. *Chem. Cat. Chem.* **2009**, *1*, 441-444.
37. Ching, S.; Roark, J. L.; Duan, N.; Suib, S. L. *Chem. Mater.* **1997**, *9*, 750-754.
38. Chen, X.; Shen, Y.-F.; Suib, S. L.; O'Young, C. L. *Chem. Mater.* **2002**, *14*, 940-948.
39. Polverejan, M.; Villegas Josanlet, C.; Suib, S. L. *J. Am. Chem. Soc.* **2004**, *126*, 7774-5.
40. Ding, Y.-S.; Shen, X.-F.; Sithambaram, S.; Gomez, S.; Kumar, R.; Crisostomo, V. M. B.; Suib, S. L.; Aindow, M. *Chem. Mater.* **2005**, *17*, 5382-5389.
41. Villegas, J. C.; Garces, L. J.; Gomez, S.; Durand, J. P.; Suib, S. L. *Chem. Mater.* **2005**, *17*, 1910-1918.
42. Yuan, J.; Li, W.-N.; Gomez, S.; Suib, S. L. *J. Am. Chem. Soc.* **2005**, *127*, 14184-14185.
43. Chen, C. H.; Jin, L.; Espinal, A. E.; Firliet, B. T.; Xu, L. P.; Aindow, M.; Joesten, R.; Suib, S. L. *Small* **2010**, *6*, 988-992.
44. Jin, L.; Reutenauer, J.; Opembe, N.; Lai, M.; Martenak, D. J.; Han, S.; Suib, S. L. *Chemcatchem* **2009**, *1*, 441-444.
45. Cai, J.; Liu, J.; Willis, W. S.; Suib, S. L. *Chem. Mater.* **2001**, *13*, 2413-2422.
46. Luo, J.; Zhang, Q.; Garcia-Martinez, J.; Suib, S. L. *J. Am. Chem. Soc.* **2008**, *130*, 3198-3207.
47. Makwana, V. D.; Son, Y.-C.; Howell, A. R.; Suib, S. L. *J. Catal.* **2002**, *210*, 46-52.
48. Opembe, N. N.; Son, Y.-C.; Sriskandakumar, T.; Suib, S. L. *ChemSusChem* **2008**, *1*, 182-185.
49. Hu, B. X.; Stancovski, V.; Morton, M.; Suib, S. L. *Appl. Catal., A* **2010**, *382*, 277-283.
50. Sriskandakumar, T.; Opembe, N.; Chen, C.-H.; Morey, A.; King'ondu, C.; Suib, S. L. *J. Phys. Chem. A* **2009**, *113*, 1523-1530.
51. Hu, B. X.; Chen, C. H.; Frueh, S. J.; Jin, L.; Joesten, R.; Suib, S. L. *J. Phys. Chem. C* **2010**, *114*, 9835-9844.
52. Yuan, J.; Liu, X.; Akbulut, O.; Hu, J.; Suib, S. L.; Kong, J.; Stellacci, F. *Nat. Nanotechnol.* **2008**, *3*, 332-336.
53. Chen, C. H.; Njagi, E. C.; Sun, S. P.; Genuino, H.; Hu, B. X.; Suib, S. L. *Chem. Mater.* **2010**, *22*, 3313-3315.
54. Njagi, E. C.; Genuino, H. C.; King'ondu, C. K.; Chen, C. H.; Horvath, D.; Suib, S. L. *Int. J. Hydrogen Energy* **2011**, *36*, 6768-6779.
55. Njagi, E. C.; Chen, C. H.; Genuino, H.; Galindo, H.; Huang, H.; Suib, S. L. *Appl. Catal., B* **2010**, *99*, 103-110.
56. Chen, X.; Mao, S. S. *Chem. Rev.* **2007**, *107*, 2891-2959.

  